

# Large orbital magnetic moments in carbon nanotubes generated by resonant transport

Naoto Tsuji, Shigehiro Takajo,\* and Hideo Aoki

*Department of Physics, University of Tokyo, Hongo 7-3-1, Bunkyo-ku, Tokyo 113-0033, Japan*

(Received 18 December 2006; published 19 April 2007)

The nonequilibrium Green's function method is used to study the ballistic transport in metallic carbon nanotubes when a current is injected from the electrodes with finite bias voltages. We reveal, both analytically and numerically, that large loop currents circulating around the tube are induced, which come from a quantum-mechanical interference and are much larger than the current along the tube axis when the injected electron is resonant with a time-reversed pair of degenerate states, which are, in fact, inherent in the zigzag and chiral nanotubes. The loop current produces large orbital magnetic moments, making the nanotube a molecular solenoid.

DOI: [10.1103/PhysRevB.75.153406](https://doi.org/10.1103/PhysRevB.75.153406)

PACS number(s): 75.75.+a, 72.20.My, 73.23.Ad, 73.63.-b

## INTRODUCTION

Carbon nanotubes (CNTs) have remarkable electronic properties related with their unique geometrical structure.<sup>1,2</sup> For example, the way in which the graphene sheet is wound into a cylinder determines whether CNTs are metals or semiconductors.<sup>3,4</sup> Recent advances have made the measurements of electrical properties of individual single-wall CNTs possible.<sup>5,6</sup> Most recently, orbital magnetic moments of a single-wall CNT have been detected, where the presence of moment is deduced from the shift of energy levels in external magnetic fields.<sup>7-9</sup> Since the magnitude of magnetic moments estimated in the experiment is about ten times the Bohr magneton, the CNT as a molecular solenoid has attracted attention.

Semiclassically, the large orbital magnetic moments can be understood as an effect of chiral currents, for which several semiclassical calculations have been done based on Boltzmann's equation.<sup>10,11</sup> However, the approach, being applicable when the transport is diffusive and lacks coherence, cannot treat purely quantum-mechanical effects. Quantum-mechanical treatments of magnetic properties of CNTs have previously been given,<sup>12-15</sup> but those studies have concentrated on the energy shift and moment of an isolated CNT in external magnetic fields in equilibrium, so the currents and the effects of electrodes have not been studied. Since ballistic transport can be strongly affected by electrodes, we need to take account of the influence of electrodes in CNTs, which is exactly our motivation here. In the process, the quantum loop current, a purely quantum-mechanical effect, has turned out to be indeed large, which we study by making use of the nonequilibrium Green's function method.<sup>16</sup>

A loop current has been studied in the context of small molecules placed between the scanning tunneling microscope (STM) tip and the substrate. Specifically, Nakanishi and Tsukada<sup>17</sup> and Tsukada *et al.*<sup>18</sup> have shown that a loop current can be dramatically amplified when the energy of the injected electron is resonant with degenerate eigenstates of an isolated molecule. This mechanism should also be applicable to CNTs, for which a special interest is the effect of inherent degeneracies associated with wave functions traveling clockwise and anticlockwise around the tube. We develop a perturbation expansion of the nonequilibrium Green's function in the weak coupling between the conductor and electrodes. This serves to identify how the loop cur-

rent paths are determined in terms of phase variation of wave functions. The peculiarity of the CNTs appears as their band structure that can satisfy the condition for large orbital magnetic moments.

We then numerically calculate the current distribution and the magnitude of the orbital magnetic moments as a function of the bias voltage, which confirms the analytic discussions. The order of magnitude of the magnetic moment obtained in the numerical calculation is consistent with the value estimated in the experiment.<sup>7</sup> Throughout this Brief Report, we consider metallic CNTs in the absence of external magnetic fields. CNTs are characterized by the chiral index  $(n_1, n_2)$  in standard literatures,<sup>1,2</sup> where CNTs are metals when  $n_1 - n_2 \equiv 0 \pmod{3}$  or semiconductors otherwise.<sup>3,4</sup> Here, we concentrate on the one-body problem.

## FORMALISM

We employ the tight-binding model whose Hamiltonian is

$$H = H_{\text{CNT}} + H_{\text{CNT-electrode}} + H_{\text{electrode}},$$

$$H_{\text{CNT}} = -t \sum_{\langle ij \rangle \in \text{CNT}} (c_i^\dagger c_j + c_j^\dagger c_i), \quad (1)$$

$$H_{\text{CNT-electrode}} = -t' \sum_{p=s,d} (c_p^\dagger c_{p'} + c_{p'}^\dagger c_p), \quad (2)$$

$$H_{\text{electrode}} = -t'' \sum_{\langle ij \rangle \in \text{electrode}} (c_i^\dagger c_j + c_j^\dagger c_i). \quad (3)$$

Here,  $H_{\text{CNT}}$  is the tight-binding Hamiltonian for the single-wall CNT,  $H_{\text{CNT-electrode}}$  describes the connection between the CNT and the electrodes,  $H_{\text{electrode}}$  describes the electrodes,  $s, s', d, d'$  are the sites connecting the CNT and the electrodes, and  $t, t', t'' (> 0)$  are the respective transfer integrals [see Fig. 1(a)].  $t$ , the transfer integral of CNT, is  $O(1 \text{ eV})$ ,<sup>1</sup> while we have taken  $t''$  for the electrodes to be large enough so that their density of states is nearly constant (wide-band limit) and  $t'$ , the hopping between CNT and electrodes to be  $\ll t, t''$ . Here, we follow other theoretical literature in assuming electrodes to be one dimensional for simplicity.

For one-dimensional (1D) electrodes, the retarded and advanced Green's functions  $G^{R,A}(E) = (E - H \pm i\epsilon)^{-1}$

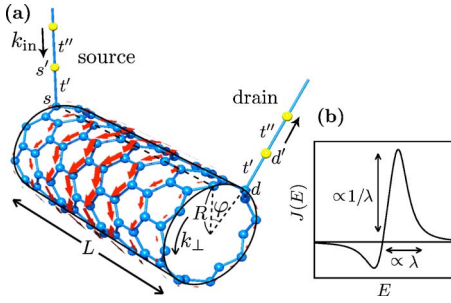


FIG. 1. (Color online) (a) A nanotube attached to 1D electrodes is schematically shown. The arrows represent the quantum loop current. (b) A typical asymmetric peak of the current density  $J_{ij}^\alpha$  vs energy.

[where  $+$  ( $-$ ) is assigned to  $R$  ( $A$ )] can be cast into a form<sup>16</sup>

$$G^{R,A}(E) = (E - H_{\text{CNT}} - \Sigma^{R,A})^{-1},$$

$$\Sigma^{R,A} = \Sigma_s^{R,A} + \Sigma_d^{R,A},$$

$$\Sigma_p^{R,A} = -\lambda t e^{\pm i k_{\text{in}} a_0} c_p^\dagger c_p \quad (p = s, d),$$

where  $\lambda = (t')^2 / (tt'')$  characterizes the sample-electrode coupling, and  $k_{\text{in}}$  the Bloch's wave number for the incident electron having an energy  $E = -2t' \cos(k_{\text{in}} a_0)$  with  $a_0$  the lattice constant of the conductor and electrodes. This reduces the problem to the sample alone, with the effects of electrodes contained in the self-energy  $\Sigma^{R,A}$ .

We can perform perturbation expansions in terms of the weak coupling  $\lambda$ . Since nonperturbative effects often arise in resonance phenomena, here we adopt the eigenfunction expansion method<sup>16</sup> that can take nonperturbative corrections into account. In this formalism we express the Green's function as  $G^R(\mathbf{r}_1, \mathbf{r}_2) = \sum_\alpha \phi_\alpha^R(\mathbf{r}_1) \phi_\alpha^{A*}(\mathbf{r}_2) / (E - E_\alpha)$ , where  $\phi_\alpha^{R,A}(\mathbf{r})$  are the eigenfunctions of the non-Hermitian operators  $H_{\text{CNT}} + \Sigma^{R,A}$  that form a biorthonormal set. The current  $I_{ij}$  flowing from site  $i$  to  $j$  is given by  $I_{ij} = \int_{\mu_d}^{\mu_s} dE J_{ij}(E)$ , where  $\mu_s$  and  $\mu_d$  are the chemical potentials of the source and drain electrodes, respectively. The current density  $J_{ij}$  per unit energy is calculated as

$$J_{ij}(E) = \frac{4e}{h} \text{Im}[H_{ij} G_{ji}^n(E)], \quad (4)$$

where  $G^n$  is the nonequilibrium Green's function defined by the usual Green's functions as  $G^n = G^R \Sigma^{\text{in}} G^A$  with  $\Sigma^{\text{in}} = i(\Sigma_s^R - \Sigma_s^A)$  at zero temperature.<sup>16,17</sup> These currents generate an orbital magnetic moment  $\mathbf{M} = \frac{1}{2} \int d\mathbf{r} \mathbf{r} \times \mathbf{j}(\mathbf{r}) = \frac{1}{2} \sum_{(ij)} I_{ij} \mathbf{r}_i \times \mathbf{r}_j$ .

Let us consider the case where the incident electron is resonant to doubly degenerate states  $\phi_1, \phi_2$  with an eigenenergy  $\varepsilon_\alpha$ . In the degenerate perturbation theory, the zeroth-order  $\phi_1^R (= \phi_1^A)$  and  $\phi_2^R (= \phi_2^A)$ , having  $E_{1,2} = \varepsilon_\alpha + \Sigma_{1,2}^R$  with  $\Sigma_{1,2}^R$  the eigenvalues of  $2 \times 2$   $\Sigma^R$ , can be written as  $(\phi_1 \pm \phi_2) / \sqrt{2}$ , respectively, where we fix  $\phi_{1,2}$  as the *time-reversed pair* with  $\phi_1 = \phi_2^* \equiv \phi_\alpha$  and choose the overall phase of  $\phi_\alpha$  so that  $[\phi_\alpha(s)]^2 + [\phi_\alpha(d)]^2$  be real. The Green's function becomes

$$\begin{aligned} G^R(i, j) &\approx \frac{\phi_1^R(i) \phi_1^{A*}(j)}{E - E_1} + \frac{\phi_2^R(i) \phi_2^{A*}(j)}{E - E_2} \\ &= 2 \left( \frac{\text{Re}[\phi_\alpha(i)] \text{Re}[\phi_\alpha(j)]}{E - \varepsilon_\alpha - \Sigma_1^R} + \frac{\text{Im}[\phi_\alpha(i)] \text{Im}[\phi_\alpha(j)]}{E - \varepsilon_\alpha - \Sigma_2^R} \right). \end{aligned} \quad (5)$$

Here, we have only retained the term related to the resonant states  $\alpha$ , which is valid as long as the splitting,  $\sim \lambda t$ , of the degenerate levels due to the self-energy is smaller than the interval across the adjacent energy level [ $\sim 1 \text{ meV}/L$  ( $\mu\text{m}$ ) for CNTs (Ref. 2)], i.e.,  $\lambda \ll 10^{-3}/L$  ( $\mu\text{m}$ ) for CNTs with  $t \sim 1 \text{ eV}$ .

From Eqs. (4) and (5), we end up with

$$\begin{aligned} J_{ij}^\alpha(E) &\approx \frac{16e}{h} \text{Im}\{[\phi_\alpha(s)]^2\} \frac{\lambda t^2 (E - \varepsilon_\alpha) \text{Im}(\Sigma_1^R - \Sigma_2^R)}{|E - \varepsilon_\alpha - \Sigma_1^R|^2 |E - \varepsilon_\alpha - \Sigma_2^R|^2} \\ &\quad \times \text{Im}[\phi_\alpha(i) \phi_\alpha^*(j)]. \end{aligned}$$

This expression can also be derived by using the results of Nakanishi and Tsukada.<sup>17</sup> We can see that the  $E$  dependence of the current density  $J_{ij}^\alpha$  is mainly determined by the factor  $(E - \varepsilon_\alpha) / (|E - \varepsilon_\alpha - \Sigma_1^R|^2 |E - \varepsilon_\alpha - \Sigma_2^R|^2)$ . This function exhibits an asymmetric peak [with width  $\sim \lambda$  and height  $\sim 1/\lambda$ , see Fig. 1(b)], which is why the integration across the peak results in a finite net current. Sasada and Hatano<sup>19</sup> has interpreted the asymmetric resonance shape for the transmission coefficient as Fano effect, i.e., an interference between continuous states in electrodes and discrete states in a conductor. So the present case may be called a *Fano effect extended to loop currents*.

## ANALYTIC EXPRESSION FOR THE CURRENT AND THE MAGNETIC MOMENT

When we integrate  $J_{ij}^\alpha(E)$  to obtain  $I_{ij}^\alpha$ , we can replace the range  $\mu_d \leq E \leq \mu_s$  with  $-\infty \leq E \leq \infty$ , since  $J_{ij}^\alpha$  is negligible outside the peak. By taking care of  $E$  dependences in  $k_{\text{in}}$  and  $\Sigma_{1,2}^R$  as well, we obtain

$$\begin{aligned} I_{ij}^\alpha &= \frac{8e t^2 \varepsilon_\alpha}{h t''} \text{Im}\{[\phi_\alpha(s)]^2\} \frac{\lambda \text{Im}[\Sigma_1^R(\varepsilon_\alpha) - \Sigma_2^R(\varepsilon_\alpha)]}{|\Sigma_1^R(\varepsilon_\alpha) - \Sigma_2^R(\varepsilon_\alpha)|^2} \\ &\quad \times \text{Im}[\phi_\alpha(i) \phi_\alpha^*(j)] + O(\lambda). \end{aligned} \quad (6)$$

Since  $\Sigma^R \sim \lambda$ , the leading term of  $I_{ij}^\alpha$  is  $\sim \lambda^0$ . This is to be contrasted with a nondegenerate resonant state  $\alpha$ , for which the corresponding expression involves the factor  $\text{Im}[\phi_\alpha(i) \phi_\alpha^*(j)]$ , but this must vanish in the absence of external magnetic fields, so the current is small [ $O(\lambda)$ ]. For the degenerate case,  $I_{ij}^\alpha \propto \text{Im}[\phi_\alpha(i) \phi_\alpha^*(j)]$  indicates that currents flow along the direction in which the phase of  $\phi_\alpha$  varies. So this implies that a cylindrical conductor, with a standing wave along the axis and a propagating wave around the tube, should have currents circulating around the tube that is *much larger* than the component flowing along the axis.

From Eq. (6), the magnetic moment along the tube axis generated by the current becomes

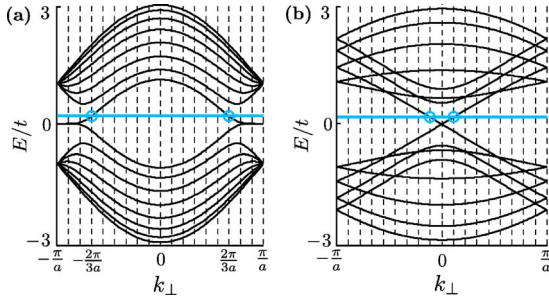


FIG. 2. (Color online) Band structure against  $k_{\perp}$  for typical (a) zigzag or (b) armchair CNTs. The vertical dashed lines indicate discrete  $k_{\perp}$  points. The horizontal line represents the energy of the incident electron.

$$\begin{aligned}
 (M_{\alpha})_z = & \frac{2e t}{\hbar} t'' \varepsilon_{\alpha} \frac{\text{Im}\{[\phi_{\alpha}^*(s)\phi_{\alpha}(d)]^2\}}{[\phi_{\alpha}(s)]^2 + [\phi_{\alpha}(d)]^2} \sum_{\langle ij \rangle} \text{Im}[\phi_{\alpha}(i)\phi_{\alpha}^*(j)] \\
 & \times (\mathbf{r}_i \times \mathbf{r}_j)_z + O(\lambda). \quad (7)
 \end{aligned}$$

The total magnetic moment is the sum over the resonant states which are relevant to transport. While  $M_{\alpha}$  is proportional to the resonant energy level  $\varepsilon_{\alpha}$ , this is only valid for 1D electrodes with Eq. (3), so the specific form should depend on the detail of the electrodes. In addition, we note that, while one might expect that edge states, which are known to exist in a finite carbon nanotube with a flat dispersion on the Fermi energy,<sup>20</sup> may have an important effect on the magnetic moment, the contribution from edge states is negligible for 1D electrodes since  $M_{\alpha} \propto \varepsilon_{\alpha}$ , as shown in Eq. (7).

Equation (7) contains a factor  $\text{Im}\{[\phi_{\alpha}^*(s)\phi_{\alpha}(d)]^2\}$ , which gives  $M_{\alpha} \propto \sin(2k_{\perp}^{\alpha} R \varphi)$  if we assume, for a heuristic purpose, a simple plane-wave form around the circumference  $\phi_{\alpha}(s) = \phi_{\alpha}^*(d) = |\phi_{\alpha}(s)| \exp(ik_{\perp}^{\alpha} R \varphi / 2)$ , where  $k_{\perp}^{\alpha}$  is the wave number around the tube of the state  $\alpha$ ,  $R$  is the radius of the tube, and  $\varphi$  is the angle subtended by the two electrodes, as shown in Fig. 1(a). Only when the electrodes are attached asymmetrically ( $\varphi \neq 0$ ) does the loop current arise, which immediately resolves a puzzle one might have on the symmetry: how a specific sense of rotation of the circulating current can arise when the cylindrical conductor has no structural chirality (as in zigzag or armchair CNTs).

The above expression for  $\mathbf{M}$  contains another factor,  $\text{Im}[\phi_{\alpha}(i)\phi_{\alpha}^*(j)] \propto \sin\{k_{\perp}^{\alpha}[\theta(i) - \theta(j)]\}$ , where we set  $\phi_{\alpha}(\mathbf{r}) = |\phi_{\alpha}(\mathbf{r})| e^{ik_{\perp}^{\alpha} \theta(\mathbf{r})}$  with  $\theta$  the coordinate along the circumference. This factor expresses that loop currents are generated due to interference between the doubly degenerate states. Since these resonant states (encircled in Fig. 2) that participate in electronic transport lie near  $\varepsilon_F = 0$ , the range of the value of  $k_{\perp}$  is determined by the band structure of the conductor in general. In particular, the metallic CNTs with  $(n_1 - n_2) \equiv 0 \pmod{3}$  have<sup>2</sup> (see Fig. 2)

$$k_{\perp} = \begin{cases} 0, & (n_1 - n_2)/n \equiv 0 \pmod{3}: \text{armchair CNT} \\ \pm \frac{2\pi}{3a}, & (n_1 - n_2)/n \not\equiv 0 \pmod{3}: \text{zigzag CNT}, \end{cases}$$

where  $n$  is the greatest common divisor of  $(n_1, n_2)$  and  $a$  the length of the translational vector along the circumference.

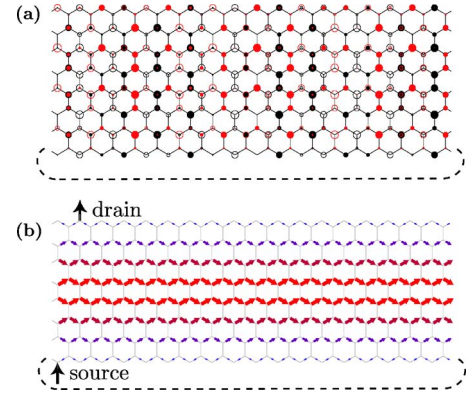


FIG. 3. (Color online) (a) Typical doubly degenerate (in black and red) eigenfunctions with an eigenenergy of  $0.419522t$  in a zigzag CNT with  $(n_1, n_2) = (18, 0)$  and  $L = 11a_0/\sqrt{3}$ .  $\circ$  and  $\bullet$  indicate the sign and the amplitude of the wave function. The dashed line indicates how the honeycomb lattice is wound into a tube. (b) A typical current distribution which is resonant to the state illustrated in (a). The size of the colored arrows indicates the magnitude of the current density, while the black arrows indicate the source and drain electrodes.

Thus, armchair CNTs with  $k_{\perp} = 0$  should have nearly zero magnetic moments, which is contrasted with zigzag CNTs for which magnetic moments are large. Chiral CNTs can have either  $(n_1 - n_2)/n \equiv 0$  or  $\not\equiv 0 \pmod{3}$ , so even chiral structures, which may naively seem to guarantee a molecular solenoid, can have large moments only when the dispersion is correct.

So we conclude that large loop currents arise when we have (i) time-reversed pair of degenerate states, (ii) asymmetrically attached source and drain electrodes, and (iii)  $k_{\perp} \neq 0$ .

## NUMERICAL RESULTS FOR CARBON NANOTUBES

We now move on to the numerical calculation to confirm the analytical discussions above. We have calculated the current and the magnetic moment for various types of CNT directly from Eq. (4) for  $t'/t = 0.2$  and  $t''/t = 2$  with  $\lambda = 0.02$ . Figure 3(a) shows typical doubly degenerate eigenstates in a zigzag CNT, while the current density resonant to the state is depicted in Fig. 3(b). We can immediately see that the current circulating around the tube is much larger than the one flowing along the axis, which endorses the discussion above.

Figure 4(a) shows the total current flowing along the axis of the CNT as the function of the bias voltage. We can see that the current along the axis is nearly discretized, which is due to the resonant tunneling from a 1D electrode through the discrete electron levels existing at regular intervals in a CNT. Figure 4(b) shows the total current circulating around the tube versus bias voltage, which is indeed larger than the current along the axis with a ratio  $\sim \lambda^{-1} \gg 1$ . The behavior consists of steps, but this time the increment of the current is not constant. This is attributed to the fact that the contribution to the current (or the orbital magnetic moment) from a pair of resonant eigenstates  $\alpha$  differs from pair to pair [ $\propto \varepsilon_{\alpha}$ , Eq. (7), for 1D electrodes].

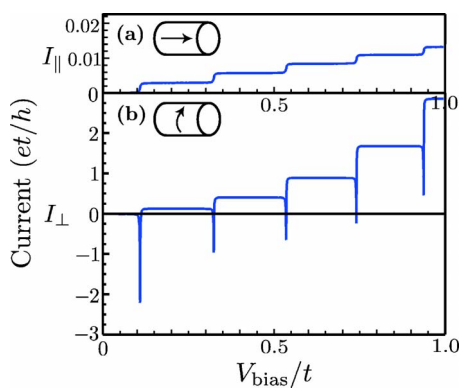


FIG. 4. (Color online) Calculated total current flowing (a) along the axis and (b) around the tube versus the bias voltage in a zigzag CNT, for which we have chosen smaller  $(n_1, n_2) = (3, 0)$  for clarity with  $L = 20a_0/\sqrt{3}$  with the same asymmetry ( $R\varphi$ ) in the electrodes as in Fig. 3(b). Note the different vertical scales.

### EVALUATION OF THE MAGNETIC MOMENT

Let us finally estimate the order of magnitude of the orbital magnetic moment in CNTs. From Eq. (7),  $M_\alpha \sim (e/\hbar)\varepsilon_\alpha R a_0$ . Around the Fermi energy, a CNT has a cone-like dispersion with  $\varepsilon_\alpha = [1 \text{ meV}/L (\mu\text{m})] \times \alpha$  ( $\alpha = 1, 2, \dots$ ). Summing over the energy levels between  $\mu_\alpha = V_{\text{bias}}$  and  $\mu_d = 0$ , we obtain  $M = \sum_\alpha M_\alpha \sim 10^{-3} \mu_B \times L (\mu\text{m}) \times [V_{\text{bias}} (\text{meV})]^2 \times (R/a_0)$ . This amounts to  $M \sim 10 \mu_B$  for  $L \sim 1 \mu\text{m}$ ,  $V_{\text{bias}} \sim 30 \text{ meV}$ , and  $R \sim 10a_0$ . We also consider the magnetic field  $B_{\text{ind}}$  generated by the circulating currents. We must satisfy  $\mathbf{M} \cdot \mathbf{B}_{\text{ind}} = M(\mu_0/2\pi R)(M/\pi R^2) \ll \lambda t$  for the energy shift due to this to be negligible. If we combine this

with the previous condition, we have to have  $[L (\mu\text{m})]^2 (R/a_0)^{-1} [V_{\text{bias}} (\text{eV})]^4 \ll \lambda \ll 10^{-3} [L (\mu\text{m})]^{-1}$  for  $t \sim 1 \text{ eV}$ . For  $V_{\text{bias}}$  and  $R$  assumed above, the above set of inequalities is satisfied for  $L \lesssim 1 \mu\text{m}$ .

### DISCUSSIONS

Here, we have concentrated on the one-body problem. The effects of the electron-electron interaction appear in, e.g., Coulomb blockade<sup>5,6</sup> and Tomonaga-Luttinger liquid state.<sup>21</sup> So we need to take the interaction into account to describe the real systems more accurately, which is a future problem. Another point is that, although the self-induced magnetic field is small as mentioned above, some CNTs have large magnetic susceptibility,<sup>12</sup> so its effect may be an interesting problem. Also assumed is that each electrode touches only one atom of the CNTs. We have checked that the loop current is not significantly affected even when each electrode touches more than one atoms in the CNT.

Although orbital magnetic moments of CNTs come to be detected indirectly from the shift of energy levels in external magnetic fields, some direct experimental observation is desirable. We may be able to use the STM (Ref. 22) to probe the loop current or attach electrodes to CNT ropes or “forest”<sup>23</sup> to detect the overall magnetization. For the latter, some statistical average may have to be involved.

### ACKNOWLEDGMENTS

We wish to thank illuminating discussions with Seigo Tarucha, Tsuneya Ando, and Takashi Oka. This work was in part supported by a Grant in Aid for Creative Scientific Research Project from the Japanese Ministry of Education.

\*Present address: Institute for Solid State Physics, University of Tokyo, Kashiwa, Chiba 277-8582, Japan.

<sup>1</sup>R. Saito, G. Dresselhaus, and M. S. Dresselhaus, *Physical Properties of Carbon Nanotubes* (Imperial College Press, London, 1998).

<sup>2</sup>S. Reich, C. Thomsen, and J. Maultzsch, *Carbon Nanotubes: Basic Concepts and Physical Properties* (Wiley-VCH, Berlin, 2003).

<sup>3</sup>N. Hamada, S. I. Sawada, and A. Oshiyama, Phys. Rev. Lett. **68**, 1579 (1992).

<sup>4</sup>R. Saito, M. Fujita, G. Dresselhaus, and M. S. Dresselhaus, Phys. Rev. B **46**, 1804 (1992).

<sup>5</sup>M. Bockrath *et al.*, Science **275**, 1922 (1997).

<sup>6</sup>S. J. Tans *et al.*, Nature (London) **386**, 474 (1997).

<sup>7</sup>E. D. Minot *et al.*, Nature (London) **428**, 536 (2004).

<sup>8</sup>U. C. Coskun *et al.*, Science **304**, 1132 (2004).

<sup>9</sup>S. Zaric *et al.*, Science **304**, 1129 (2004).

<sup>10</sup>Y. Miyamoto, S. G. Louie, and M. L. Cohen, Phys. Rev. Lett. **76**, 2121 (1996).

<sup>11</sup>O. M. Yevtushenko, G. Y. Slepyan, S. A. Maksimenko, A. Lakhtakia, and D. A. Romanov, Phys. Rev. Lett. **79**, 1102 (1997); G. Y. Slepyan, S. A. Maksimenko, A. Lakhtakia, O. M. Yevtush-

enko, and A. V. Gusakov, Phys. Rev. B **57**, 9485 (1998).

<sup>12</sup>H. Ajiki and T. Ando, J. Phys. Soc. Jpn. **62**, 2470 (1993).

<sup>13</sup>T. Ando, J. Phys. Soc. Jpn. **74**, 777 (2005).

<sup>14</sup>J. P. Lu, Phys. Rev. Lett. **74**, 1123 (1995).

<sup>15</sup>M. Margañska, M. Szopa, and E. Zipper, Phys. Rev. B **72**, 115406 (2005).

<sup>16</sup>S. Datta, *Electronic Transport in Mesoscopic Systems* (Cambridge University Press, Cambridge, 1995).

<sup>17</sup>S. Nakanishi and M. Tsukada, Jpn. J. Appl. Phys., Part 2 **37**, L1400 (1998); Surf. Sci. **438**, 305 (1999); Phys. Rev. Lett. **87**, 126801 (2001).

<sup>18</sup>M. Tsukada *et al.*, J. Phys. Soc. Jpn. **74**, 1079 (2005).

<sup>19</sup>K. Sasada and N. Hatano, Physica E (Amsterdam) **29**, 609 (2005).

<sup>20</sup>K. Nakada, M. Fujita, G. Dresselhaus, and M. S. Dresselhaus, Phys. Rev. B **54**, 17954 (1996).

<sup>21</sup>M. Bockrath *et al.*, Nature (London) **397**, 598 (1999).

<sup>22</sup>J. W. G. Wildöer *et al.*, Nature (London) **391**, 59 (1998); T. W. Odom, J. -L. Huang, P. Kim, and C. M. Lieber, *ibid.* **391**, 62 (1998).

<sup>23</sup>K. Hata *et al.*, Science **306**, 1362 (2004).